Across-vendor standardization of semi-LASER for single-voxel MRS at 3 Tesla

Dinesh K Deelchand[1,*], Adam Berrington[2,*,¥], Ralph Noeske[3], James M Joers[1], Arvin Arani[4], Joseph Gillen[2], Michael Schär[2], Jon-Fredrik Nielsen[5], Scott Peltier[5], Navid Seraji-Bozorgzad[5], Karl Landheer[6], Christoph Juchem[6], Brian J Soher[7], Douglas C Noll[5], Kejal Kantarci[4], Eva M Ratai[8], Thomas H Mareci[9], Peter B Barker[2,10], Gülin Öz[1]

[1] Center for Magnetic Resonance Research, Department of Radiology, University of Minnesota, Minneapolis, MN, USA
[2] The Russell H. Morgan Department of Radiology and Radiological Science, The Johns Hopkins University, Baltimore, MD, USA
[3] GE Healthcare, Berlin, Germany
[4] Department of Radiology, Mayo Clinic, Rochester, MN, USA
[5] Department of Biomedical Engineering, University of Michigan, MI, USA
[6] Departments of Biomedical Engineering and Radiology, Columbia University, New York, NY, USA
[7] Center for Advanced Magnetic Resonance Development, Duke University Medical Center, Durham, NC, USA
[8] Department of Radiology, Massachusetts General Hospital, Athinoula A. Martinos Center for Biomedical Imaging, Harvard Medical School, Boston, MA, USA.
[9] Department of Biochemistry and Molecular Biology, University of Florida, Gainesville, FL, USA
[10] The Kennedy Krieger Institute, Baltimore, MD, USA
¥ Current address: Sir Peter Mansfield Imaging Centre, School of Physics and Astronomy, University of Nottingham, Nottingham, UK
*Share equal authorship

Short title: Harmonization of single-voxel sLASER

Word Count: 4112

Corresponding author:
Dinesh K. Deelchand, PhD
Center for Magnetic Resonance Research, University of Minnesota
2021 6th St SE, Minneapolis, MN 55455, USA
Phone: (1) 612-625-8097; Fax: (1) 612-626-2004
Email: deelc001@umn.edu

Abstract

The semi-adiabatic localization by adiabatic selective refocusing (sLASER) sequence provides single-shot full intensity signal with clean localization and minimal chemical shift displacement error and was recommended by the international MRS Consensus Group as the preferred localization sequence at high- and ultra-high fields. Across-vendor standardization of the sLASER sequence at 3 Tesla has been challenging due to the B_1 requirements of the adiabatic inversion pulses and maximum B_1 limitations on some platforms. The aims of this study were to design a short-echo sLASER sequence that can be executed within a B_1 limit of 15 µT by taking advantage of gradient-modulated RF pulses, to implement it on three major platforms and to evaluate the between-vendor reproducibility of its perfomance with phantoms and *in vivo*. In addition, voxel-based first and second order B_0 shimming and voxel-based B_1 adjustments of RF pulses were implemented on all platforms. Amongst the gradient-modulated pulses considered (GOIA, FOCI and BASSI), GOIA-WURST was identified as the optimal refocusing pulse that provides good voxel selection within a maximum B_1 of 15 µT based on localization efficiency, contamination error and ripple artifacts of the inversion profile. An sLASER sequence (30 ms echo time) that incorporates VAPOR water suppression and 3D outer volume suppression was implemented with identical parameters (RF pulse type and duration, spoiler gradients and inter-pulse delays) on GE, Philips and Siemens and generated identical spectra on the GE 'Braino' phantom between vendors. High-quality spectra were consistently obtained in multiple regions (cerebellar white matter, hippocampus, pons, posterior cingulate cortex and putamen) in the human brain across vendors (5 subjects scanned per vendor per region; mean signal-to-noise ratio > 33; mean water linewidth between 6.5 Hz to 11.4 Hz). The harmonized sLASER protocol is expected to produce high reproducibility of MRS across sites thereby allowing large multi-site studies with clinical cohorts.

Keywords:

Brain, clinical, GOIA-WURST, gradient-modulated, human, harmonization, MR spectroscopy.

Introduction

The international Magnetic Resonance Spectroscopy (MRS) Consensus Group has recently documented the clinical utility of proton MRS in central nervous system disorders[1]. In addition, the group emphasized the critical need for standardization of advanced MRS methods to improve between-site reproducibility of data quality and metabolite quantification. In a follow-up technical consensus statement, the group concluded that the localization error for the most widely utilized conventional localization sequence point resolved spectroscopy (PRESS),[2] was unacceptably high at 3T and recommended use of the semi-adiabatic localization by adiabatic selective refocusing (sLASER) sequence at high fields (≥3T) to minimize chemical shift displacement error (CSDE)[3].

The sLASER sequence[4,5] provides single-shot full intensity signal with sharp slice selection profiles, minimal CSDE due to the high bandwidth of adiabatic full-passage (AFP) pulses at high field, and utilizes pairs of AFP pulses that act as a Carr-Purcell pulse train[6] to suppress *J*-evolution and prolong the apparent transverse (T_2) relaxation times[7,8]. The improvements in localization, spectral quality and repeatability with an sLASER vs. a conventional vendor-provided PRESS protocol were recently demonstrated[9]. Studies[10-12] using sLASER at 3T and 7T have further shown the feasibility of obtaining highly reproducible neurochemical profiles with test-retest coefficients of variance (CoV) below 5% at both field strengths for the five major metabolites: total *N*-acetylaspartate (tNAA), total creatine (tCr), total choline (tCho), glutamate (Glu) and *myo*-inositol (Ins). Finally, good between-site reproducibility was demonstrated with sLASER on 3T scanners from the same vendor[13] and on 7T scanners from two vendors[14].

However, standardization of the sLASER sequence across three major clinical platforms (GE, Philips and Siemens) has been challenging at 3T due to the high B_1 field requirements of the AFP pulses. In addition, there are software constraints imposed by some vendors on the maximum available B_1. These can depend on the coil configuration, transmission modes and the particular method in question. The challenges presented by such explicit B_1 constraints can be alleviated by using gradient-modulated RF pulses[15]. These pulses require lower peak power than conventional hyperbolic secant pulses used in the original LASER[16] and sLASER[4,5] implementations and therefore reduce SAR deposition especially at high fields. Commonly used gradient-modulated

RF pulses include Bandwidth-modulated Adiabatic Selective Saturation and Inversion (BASSI)[17], Frequency Offset Corrected Inversion (FOCI)[18] and Gradient Offset Independent Adiabatic (GOIA)[15,19] RF pulses.

Therefore, the aims of the current study are 1) to design a short-echo single-voxel sLASER sequence that can be executed within a conservative maximum B_1 field of 15 µT at 3T by taking advantage of gradient-modulated RF pulses, 2) to implement sLASER with identical parameters (RF pulse type and duration, spoiler gradients and inter-pulse delays) on GE, Philips and Siemens, 3) to implement voxel-based first and second order B_0 shimming and voxel-based B_1 calibration of RF pulses on all platforms and 4) to evaluate the performance of this advanced MRS protocol by acquiring spectra on phantoms and in the human brain *in vivo* in multiple volumes-of-interest (VOI) relevant to neurological and psychiatric diseases.

Methods

Selection of the refocusing RF pulse

The modified sLASER sequence proposed by Öz and Tkáč at 4T[5] originally used a 3.5 ms adiabatic refocusing pulse (4^{th} order hyperbolic secant, 7.14 kHz bandwidth) denoted as HS4R25 and required a maximum B_1 of 29 µT at 4T. At 3T the duration of this pulse was lengthened to 4 ms requiring a maximum B_1 of ~25 µT (6.25 kHz bandwidth)[10,13]. BASSI[17], FOCI based on C-shaped modulation[18] and two types of GOIA based on hyperbolic secant (GOIA-HS)[19] and WURST (GOIA-WURST)[15] modulation adiabatic pulses were considered (Figure 1) as potential alternatives to the HS4R25 refocusing pulse.

These four gradient-modulated pulses were generated in MATLAB R2013b (MathWorks, Natick, MA, USA). To systematically evaluate the RF pulses, Bloch simulations were run with various pulse durations, bandwidth and waveform modulations until at least 98% magnetization inversion (Mz) was obtained. These simulations were perfomed with a constraint to the maximum available B_1 of 15 µT, since this was the limit across the platforms in our study. In particular, the limit on maximum B_1, using the dual transmit body coil on the Philips system, was increased from its default value of 13.5 µT to 15 µT with permission from the vendor. It is noted, however, that higher limits are now available (22 µT) on Philips systems when using certain advanced

applications such as multi-band. The 15 μT limit in this study was the maximum available at the time of the study and represents a value that the majority of 3T Philips users who use the dual-transmit body coil can achieve, without needing any advanced software updates. On GE and Siemens platforms, the maximum B_1 is between 20 to 25 μT. The performance of the selected pulses was assessed by measuring the localization efficiency inside the desired inversion profile, contamination error outside the inversion profile and ripple artifacts. These metrics were evaluated both on resonance and 200 Hz off-resonance. 200 Hz was chosen to observe the effect of frequency offset on the furthest metabolites at 4.3 ppm with the carrier frequency set at 2.67 ppm.

Localization efficiency was defined as the ratio of magnetization inverted inside the targeted VOI to an ideal rectangular profile and was expressed $L_{Eff} = A_{in}/I_{in}$ where A_{in} is the area-under-the-curve (AUC) of the M_z profile for an actual RF pulse and I_{in} is the AUC for an ideal rectangular waveform (Suppl. Figure 1). Similarly, the contamination error was defined as $C_{Err}=A_{out}/A_{in}$ where A_{out} is the AUC of the M_z profile outside the ideal profile (Suppl. Figure 1). The ripple artifact was evaluated by measuring the peak-to-peak ripple (R_{PP}) and is defined as the difference between the minimum and maximum magnetization measured both inside (Mz = -1, pass-band) and outside (Mz = 1, stop-band) the targeted VOI (Suppl. Figure 1) and is expressed as a % of Mz. Therefore a lower value indicates a smaller artifact.

CSDE in %/ppm was determined using the simulated M_z profiles at 0 and 123 Hz (i.e. 1 ppm at 3T) and was calculated as (VOI_{shift}/VOI_{size}) where VOI_{shift} is the spatial displacement of the VOI at an offset of 123 Hz relative to 0 Hz and VOI_{size} is the VOI dimension used in simulation (i.e. 2 cm in the current study).

Multi-vendor pulse sequence implementation

The modified sLASER sequence was implemented with the same parameters (RF pulse type and duration, spoiler gradients and inter-pulse delays) on GE, Philips and Siemens 3T platforms (Figure 2). Identical excitation pulses were used (2.6 ms duration, 2.6 kHz bandwidth), which were asymmetric[20], and were implemented together with the refocusing pulses determined from simulations (as described above). Based on the duration of the RF pulses (Table 1), the inter-pulse

durations between the pulses were also matched between scanners. The ramp time for all gradients was set to 200 µs with a maximum crusher strength of 34 mT/m in sLASER. The phase cycling scheme[5] as originally proposed was used (Supplementary Table 1).

Water suppression was achieved with VAPOR[20] interleaved with outer volume suppression pulses (OVS). A 30 ms SLR pulse (70 Hz bandwidth) was used for water suppression with the following inter-pulse delays (in ms): 160 – 110 – 132 – 115 – 112 – 71 – 88 – 22. Three pairs of OVS pulses with variable RF powers were applied in the direction selected by the slice-selective excitation pulse to eliminate signal arising from outside the VOI due to the sidebands of the 90° pulse (Figure 2). Based on the cleaner slice-selection profiles of the AFP pulses, a single OVS module was used to suppress unwanted coherences in the AFP directions[5]. The OVS pulse used on GE and Siemens scanners was a 5.12 ms hyperbolic secant pulse (7.8 kHz bandwidth), while on Philips an 8 ms hyperbolic secant pulse (3 kHz bandwidth) was used due to a lower constrained maximum B_1. The crusher gradients used in the VAPOR/OVS schemes ranged from 1 to 10 ms in duration and from 1 to 20 mT/m in amplitude.

In vitro and *in vivo* measurements

Four institutions with 3T MR scanners from the major vendors participated in this study: Philips Ingenia Elition scanner (MR Release 5.5.2 DDAS SWID114 software) located at the Kennedy Krieger Institute (KKI), GE Discovery MR750 scanner (DV26 software) located at the University of Michigan and Siemens Prisma scanners (Syngo MR VE11C software) located at the University of Minnesota and Mayo Clinic Rochester. All systems were equipped with the vendors' standard body coil for RF transmission and a 32-channel head array coil for signal reception (GE: Nova coil (Nova Medical Inc, Wilmington, MA); Philips and Siemens: vendor's standard coil).

For *in vitro* comparison between systems, MRS data were acquired from an 8 mL VOI at isocenter in a standard spectroscopic 'Braino' phantom[21] located at each site (General Electric, Milwaukee, WI) with 64 averages (TR/TE=3000/30 ms, the number of complex points = 2048) after performing calibrations of the B_0 and B_1 fields for each VOI as described below. The spectral width was matched as close as possible and was 6024 Hz on GE, 6000 Hz on Philips and 6002.4 Hz on

Siemens. This spectral width was chosen to avoid any effects on the baseline at the edges of the spectrum due to digital filters on the Siemens scanner.

Four groups of five healthy volunteers (University of Michigan: age = 27±11, 2 F; Johns Hopkins/KKI: age = 36±11, 1 F; University of Minnesota: age = 35±12, 1 F; Mayo Clinic: age = 37 ±2, 2 F) were recruited at each institution after giving informed consent according to procedures approved by the respective Institutional Review Board. sLASER proton spectra (TR/TE=5000/30ms; 64 averages) were acquired from 5 different brain regions: cerebellar white matter (CBWM) (17×17×17 mm^3), left hippocampus (13×26×12 mm^3), pons (16×16×16 mm^3), posterior cingulate cortex (PCC) (20×20×20 mm^3) and putamen (10×25×11 mm^3). Voxels were automatically prescribed using AutoVOI[22] to achieve reproducible voxel placement across sites. In addition to metabolite spectra, water reference scans were acquired by turning off the water suppression RF pulse for eddy current correction.

B_0 shimming for each VOI was achieved by optimizing the first and second order shim terms using the vendor-provided shimming routine on Philips (Pencil Beam) and using the system 3D gradient-echo shim, operated in the "brain" shim mode, or FASTMAP shimming[23,24] on Siemens. On the GE scanner, second order shimming is generally not done for single voxel MRS, therefore a FASTMAP like tool called FAMASITO[25,26], implemented by investigators at Columbia University, was used to adjust second order shim terms.

For each VOI, the B_1 levels for the RF pulses in sLASER and for water suppression were calibrated on each system: on the GE scanner two off-resonance Bloch-Siegert pulses were added in the sLASER sequence to determine the flip angle inside the voxel[27], on the Philips scanner the vendor-provided power optimization routine was used to calibrate the flip angle over a slice intersecting the voxel[28], on the Siemens scanner the RF power was determined by monitoring the water signal intensity from the VOI when increasing the RF power and automatically choosing the setting that produced the maximum signal[13]. The center frequency was set to 2.67 ppm for all metabolite acquisitions while this value was set to 4.67 ppm for water scans.

Raw MRS data from all sites were saved for offline post-processing using MRspa[29] in MATLAB. Data from each receive channel were combined after correcting for phase differences between

the channels and weighting them based on the coil sensitivities[30]. The resulting FIDs (64 transients per VOI) were processed as follows: eddy current correction followed by shot-to-shot frequency and phase correction before summing the spectra.

Signal-to-noise ratio (SNR) was calculated as the ratio of the tNAA peak divided by the root-mean-square noise (measured between –2 and –12 ppm) after correction for baseline offset in the frequency domain. The linewidth of the unsuppressed water signal was measured at full width at half maximum after eddy current and baseline corrections and zero-filling (to 10 times the number of points) to increase the digital resolution of the peak. Spectral linewidth of water and SNR between vendors were compared using one-way ANOVA. To correct for multiple testing (5 VOIs per 3 vendors), the threshold of significance (Bonferroni correction) was set to 0.0033 (i.e. 0.05/15).

Metabolite quantification was preliminarily compared across-vendors with the analysis limited to one VOI due to the small sample size in the study. The PCC was chosen for this analysis due to the highest SNR and narrowest water linewidth achieved in this VOI amongst the five regions studied, thus providing the highest power to detect systematic vendor differences. Metabolites were quantified using LCModel[31] version 6.3-0G (Stephen Provencher Inc, Oakville, Ontario, Canada). The basis set consisted of 19 metabolites and a measured macromolecule spectrum as previously reported[13]. Concentrations of the most prominent metabolites (tNAA, tCho, Ins, Glu, Gln) are reported relative to tCr since not all sites acquired a water reference scan with OVS turned off (to avoid magnetization transfer effects[5]) needed to estimate mM concentrations. Concentration ratios and Cramér-Rao Lower Bounds (CRLB) were compared between vendors for reported metabolites using one-way ANOVA. To correct for multiple testing for concentrations and CRLBs, the threshold of significance was set to 0.0033 (i.e. 0.05/15 for 5 metabolites and 3 pair-wise across-vendor comparisons)and 0.0028 (i.e. 0.05/18 for 6 metabolites and 3 pair-wise across-vendor comparisons), respectively.

Results

Assessment of gradient-modulated RF pulses

Based on the measurements of simulated inversion profiles, several gradient-modulated RF pulses with appropriate parameters (given in Table 1) were found to satisfy the requirement of at least 98% inversion at a maximum B_1 of 15 μT with a duration of 4.5 ms. For GOIA-HS and GOIA-WURST, a bandwidth of 10 kHz was found to be sufficient to invert 98% of the magnetization while for FOCI 98% inversion was achieved with a bandwidth of 8.89 kHz. For BASSI, several parameters such as β=2.7 rad, κ = 2, b_0 = 10.5 rad and f_0 = 8.03 (as defined in the original paper[17]) were adapted to produce a 10 kHz bandwidth. CSDE for these gradient-modulated pulses was ≤ 2 %/ppm, with FOCI having the lowest CSDE of < 1%/ppm (Table 1).

These selected RF pulses were further evaluated for localization performance. On resonance, the FOCI pulse had the highest inversion efficiency (96.6%) followed by BASSI, GOIA-WURST and GOIA-HS (Table 2). The FOCI pulse displayed the sharpest transition in the Mz profile (Figure 3). In addition, the contamination error was less than 5% for all four gradient-modulated pulses, with the FOCI pulse having the lowest contamination error of 2.3% on resonance. Therefore the FOCI pulse outperformed the other pulses for CSDE, inversion efficiency, sharpness of the Mz transition and contamination error. However, it displayed worse ripple artifacts than GOIA-WURST, both inside and outside the targeted VOI. The ripple artifact inside the VOI was lowest for GOIA-WURST (1.77%) and highest for BASSI (11.8%). Outside the VOI, the ripple artifact was lowest and comparable for both GOIA pulses.

For the off-resonance condition at 200 Hz, the inversion efficiency ranged between 93 - 95% and this was slightly lower compared to the on resonance case (Table 2). As expected, the ripple artifact was more pronounced off-resonance for these RF pulses, with GOIA-WURST showing the lowest artifact error inside and outside the VOI amongst the different gradient-modulated pulse types.

Based on these measured metrics, the 4.5 ms GOIA-WURST (10 kHz bandwidth) was chosen as the refocusing pulse in the harmonized sLASER sequence. This pulse was preferred over the FOCI pulse due to minimal ripple artifacts observed both inside and outside the VOI, on- and off-resonance, in addition to clean localization. To accommodate the GOIA-WURST pulse, the inter-pulse durations in sLASER were adjusted to be 8, 12 and 10 ms for TE1, TE2 and TE3 delays,

respectively, such that the final echo time (TE) was 30 ms. The standardized sLASER sequence with the selected GOIA-WURST pulses is shown in Figure 2.

In vitro spectral quality

Spectra acquired from the standard 'Braino' phantom on each platform are shown in Figure 4. Markedly similar spectral profiles were observed between vendors confirming that identical implementation and performance of the sLASER sequence was achieved across platforms. The water linewidth was between 3.3 to 3.8 Hz. Similarly, comparable SNR (ranging from 447 to 490) was observed between scanners.

In vivo comparison

The mean (± SD) *in vivo* spectra acquired from all subjects on the three platforms are shown in Figure 5. Spectral quality and pattern were highly reproducible between individuals and platforms in all studied brain regions with minimal baseline artifacts and unwanted coherences across scanners. The signal variation observed around 4.2 ppm in the hippocampus and pons data on the GE platform was related to inefficient water suppression in one subject.

Spectra obtained from the PCC had the narrowest linewidth, with water linewidths between 6.3 Hz to 7.3 Hz across vendors in all subjects, amongst the five brain regions studied (Figure 6). No statistically significant difference in water linewidth was observed across VOIs and vendors, although the linewidth for hippocampus, pons and putamen tended to be higher on the GE platform.

Similarly, the SNR in PCC was the highest (> 140) among the studied VOIs (Figure 6) and significantly higher by ~50% on Siemens compared to GE and Philips scanners. The SNR in the hippocampus was also significantly different between GE and Siemens scanners. For other brain regions, the SNR was comparable across vendors.

The concentration of Gln, Glu, Ins, tCho, and tNAA relative to tCr in PCC are reported in Figure 7. Comparable relative concentrations were obtained between platforms. Similarly, the mean CRLB of Gln, Glu, Ins, tCr, tCho, and tNAA (Figure 7) were comparable and < 6% on all vendors, except

for Gln where the CRLB was <25%. No statistically significant difference in relative concentration and CRLBs were observed across vendors.

Discussion

This study shows the feasibility to standardize the sLASER sequence on three major clinical platforms (GE, Philips and Siemens) at 3T. An sLASER sequence using optimized GOIA-WURST refocusing pulses resulted in high-quality and reproducible spectra with comparable spectral linewidths and SNR across the different vendors in various regions of the human brain. In addition, this sequence could be implemented within a conservative constraint on the maximum B_1 field. This is an important step towards harmonizing advanced single-voxel MRS on clinical scanners as recommended by the MRS consensus group[1].

The implementation of sLASER on the three platforms was only possible due to a multi-site effort undertaken at various institutions to collaborate on this project. In order to implement the pulse sequence identically between vendors, we matched the duration and strength of all the spoiler and rephasing gradients, the type and duration of RF pulses used for excitation and refocusing, the timings between RF pulses (i.e. inter-pulse delays) and the acquisition parameters (number of complex points and spectral width). In addition, the VAPOR water suppression module and interleaved OVS pulses were matched across systems. Note that although it was necessary to have a lower bandwidth of the hyperbolic secant OVS pulse on the Philips system, this should not affect the overall localization performance of sLASER. Namely, a large CSDE associated with a small OVS bandwidth would suppress signals inside the sLASER VOI, thereby reducing the overall dimension of the VOI. However, the bandwidth of the Philips OVS pulse used here was still sufficiently large to minimize the CSDE associated with OVS (4.1 %/ppm). A standardized TE of 30 ms was selected in sLASER, similar to the vendor provided PRESS sequence. However, sLASER provides improved localization and reduced signal loss due to *J*-modulation compared to PRESS[9]. This sLASER sequence is currently available on several software versions of the vendors' platforms and is distributed through a Customer-to-Customer sequence transfer (C2P) agreement on Siemens[32], as a work-in-progress (WIP) package under a Research Software Access License on GE and through contact with the authors (AB or PBB) as a software patch to sites with

an existing Philips Research Agreement. The harmonization of data acquisition across sites will further allow centralized analysis using the same basis set and is expected to result in high between-vendor reproducibility of neurochemical concentrations[13,14].

The GOIA-WURST pulse provided the best voxel selection within the B_1 limit of 15 µT at 3T based on the simulations of inversion profile and comparison to other gradient-modulated RF pulses BASSI, FOCI and GOIA-HS investigated in this study. As expected with the large bandwidth of adiabatic pulses, the CSDE of GOIA-WURST was minimal (≤2 %/ppm) and well within the recommended maximum CSDE of 4 %/ppm by the MRS consensus group[3]. However, one of the disadvantages of gradient-modulated pulses is that at off-resonance they suffer from smearing artifacts[15]. This effect was small for GOIA-WURST as shown by the excellent pulse profiles with minimal selection outside the targeted VOI both on- and off-resonance (Figure 3), which is very important for avoiding partial volume effects and reducing contamination from lipid signals from VOIs close to the skull.

Harmonization of voxel-based B_0 and B_1 adjustments together with sLASER localization enabled us to acquire high-quality and reproducible spectra in phantoms and the human brain on the three platforms. The phantom data in particular demonstrated an identical spectral pattern at high resolution, confirming identical *J*-evolution in the sLASER sequences across scanners. In addition, the spectral patterns obtained in 5 clinically relevant VOIs were reproducible between healthy volunteers and across platforms. We therefore expect that this protocol will generate high test-retest reproducibility of metabolite concentrations on all 3 platforms, as previously demonstrated on one or two platforms[10-12].

Both first and second order shim terms were adjusted on all platforms to have optimal B_0 shim in all brain regions. This has resulted in comparable water linewidths between regions on each platform, with the exception of hippocampus, pons and putamen on the GE scanner. Differences between shimming algorithms and the volumes over which the shim terms were adjusted, e.g. a sphere over the VOI, the actual VOI or a cube the dimensions of which are set to the largest dimension of the VOI, may have caused these linewidth differences. Such algorithmic differences are expected to primarily affect shimming performance in non-cubic VOI, such as the

hippocampus and putamen, and in VOI that are close to areas with large magnetic field inhomogeneities, such as the pons.

Comparable spectral SNR was observed between vendors for the multiple VOIs studied in the brain, except for PCC and hippocampus. Although similar spectral linewidths were observed on all platforms in PCC, the measured SNR was significantly higher on Siemens than GE and Philips scanners. This difference in SNR in PCC may be due to differences in B_1 receive properties of the head array coils used across vendors since this SNR difference was not observed in the other VOIs between scanners. On the other hand, the low SNR measured in the hippocampus VOI on the GE scanner is related to the water linewidth which was broader by ~2 Hz than what was measured on the other scanners (**Figure *5***Figure 6).

Metabolite quantification was limited to ratios of the most prominent metabolites in the VOI with the highest spectral quality in the current study due to the small sample size and since not all sites acquired the appropriate water reference scan without the OVS modules to avoid magnetization transfer effects on the water signal. This preliminary analysis demonstrated comparable quantification results across-vendors (Figure 7). Future studies will focus on quantification in the multi-site setting and with appropriate sample sizes for a robust comparison of metabolite quantification across platforms.

One potential drawback of using sLASER is in determining absolute concentrations of metabolites due to the longer TE than that achievable by STEAM and SPECIAL. In order to correct for signal losses due to relaxation at 30 ms, the intrinsic T_2 values for water and each metabolite measured under Carr-Purcell (CP) conditions are required. Note that T_2 can also be different in the same molecule e.g. between CH_2 and CH_3 in tCr and between the singlet and multiplet in *N*-acetylaspartate[33]. Measurements of T_2 under CP conditions have been limited to singlets only[8], preventing accurate T_2 correction of all reported metabolite levels. Instead of absolute quantification, metabolite concentrations can be reported after only correcting for the T_2 of water[13].

Conclusion

Standardization of sLASER provided consistent and high-quality spectra between vendors across different sites. This will therefore allow pooling of data across platforms and enable MRS studies on large multi-site cohort studies and clinical trials. This sequence could also be used as a basis for standardizing other MRS sequences such as editing and magnetic resonance spectroscopic imaging. Future studies should aim to harmonize first and second order B_0 shimming algorithms and compare neurochemical profiles and test-retest reproducibility in healthy volunteers and clinical cohorts aross vendors.

Acknowledgements

This work was supported by funding from the National Institutes of Health (NIH) (R01 NS080816, P41 EB015894, P30 NS076408). The authors would like to thank Dr. Lynn Eberly for statistical consultation.

Figure Captions

Figure 1

Four different types of gradient-modulated RF pulses (BASSI, FOCI, GOIA-HS and GOIA-WURST) were compared to the hyperbolic secant HS4R25 pulse. The normalized absolute amplitude, frequency (in kHz) and normalized gradient waveforms are shown for each of these pulses. For display purposes, all pulses were simulated using a 4 ms duration and a bandwidth of 6.25 kHz for HS4R25, 11.25 kHz for BASSI and 9.5 kHz for FOCI, GOIA-HS and GOIA-WURST.

Figure 2

The schematic of the sLASER pulse sequence where the standard adiabatic refocusing pulses (HS4R25) were replaced by gradient-modulated GOIA-WURST pulses (red line). Water suppression was achieved using VAPOR with interleaved OVS pulses (three pairs in the X direction and a single pair in the Y and Z directions). The duration of these refocusing pulses was 4.5 ms and they require a B_1 of 15 µT at 3T. For standardization between the different vendors, the echo time was matched to 30 ms where the inter-pulse delays TE1, TE2 and TE3 were 8, 12 and 10 ms respectively.

Figure 3

Simulated Mz profiles for the selected RF pulses based on parameters given in Table 1. Inversion profiles are shown for on (top) and off (bottom) resonance (200 Hz or ~1.6 ppm at 3T) conditions. Insets show the zoomed in band-pass (magenta box) and band-reject (green box) regions. On resonance, all pulses achieved at least 98% inversion at a B_1 of 15 µT. As expected a larger smearing effect was observed for gradient modulated pulses for the off-resonance case compared to the HS4R25 pulse. Note that the transition band was less steep for HS4R25 compared to the gradient-modulated pulses. At -200 Hz or at 1.0 ppm, the off-resonance artifacts will be a mirror image of the M_z profile at 200 Hz (not shown).

Figure 4

'Braino' phantom spectra (64 averages) acquired from GE, Philips and Siemens MR scanners. Data were line-broadened with Gaussian multiplication of 0.12 s and 1 Hz exponential functions and normalized to the tNAA singlet (for display purposes). Identical spectral patterns were observed between vendors as illustrated by the mean (dark blue) and SD (gray) spectrum. The SNR (with respect to tNAA peak) and water linewidth (in Hz) are also reported in parentheses.

Figure 5

Mean (blue) and SD (gray) of the sLASER spectra (TE=30ms, TR=5s, 64 averages) acquired from five brain regions on GE, Philips and Siemens 3T scanners across all 5 different subjects on each scanner. Voxel locations (yellow) are shown on the T_1-weighted images. All spectra were normalized to the tNAA peak. For display purposes, a Gaussian multiplication of 0.12 s was applied. The large variation in hippocampus and pons was related to inefficient water suppression in one subject in both regions.

Figure 6

Standard box plot of water linewidth and SNR (with respect to tNAA peak) measured from five brain regions on the three major scanners (5 subjects per platform). The central red line on each box indicates the median while the the bottom and top edges indicate the 25^{th} and 75^{th} percentiles, respectively. The whiskers represent the most extreme data points. * represents $P < 0.0033$ (one-way ANOVA).

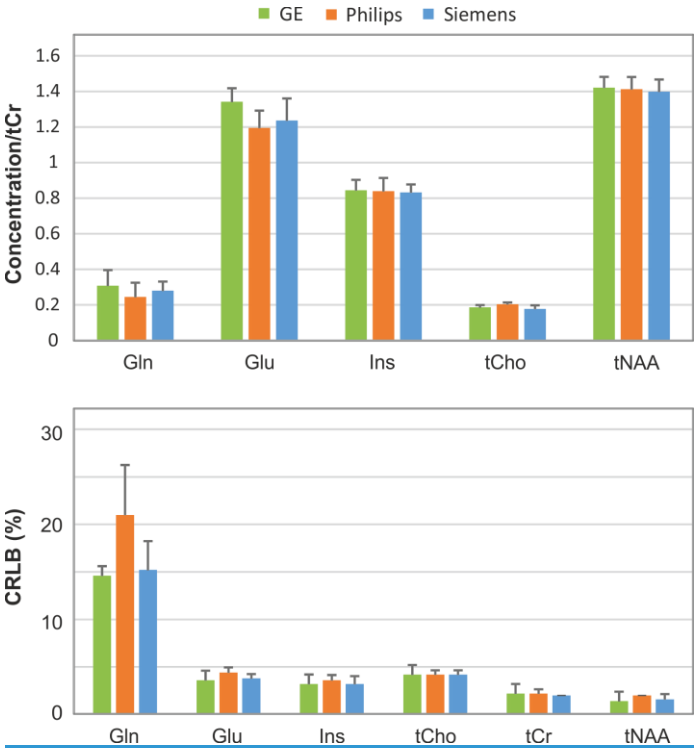

Figure 7

Mean concentrations of the most prominent metabolites relative to tCr and CRLB as measured in PCC (5 subjects per platform). Error bar represent standard deviation. No statistically significant difference (one-way ANOVA) in concentrations and CRLBs were observed between platforms.

References

1. Öz G, Alger J, Barker P, et al. The MRS Consensus Group. Clinical Proton MR Spectroscopy in Central Nervous System Disorders. *Radiology.* 2014;270(3):658-679.
2. Bottomley PA. Spatial Localization in NMR Spectroscopy in Vivo. *Ann NY Acad Sci.* 1987;508(1):333-348.
3. Wilson M, Andronesi O, Barker PB, et al. Methodological consensus on clinical proton MRS of the brain: Review and recommendations. *Magnetic Resonance in Medicine.* 2019;82(2):527-550.
4. Scheenen TWJ, Klomp DWJ, Wijnen JP, Heerschap A. Short echo time 1H-MRSI of the human brain at 3T with minimal chemical shift displacement errors using adiabatic refocusing pulses. *Magn Reson Med.* 2008;59(1):1-6.
5. Öz G, Tkac I. Short-echo, single-shot, full-intensity proton magnetic resonance spectroscopy for neurochemical profiling at 4 T: Validation in the cerebellum and brainstem. *Magn Reson Med.* 2011;65(4):901-910.
6. Carr HY, Purcell EM. Effects of Diffusion on Free Precession in Nuclear Magnetic Resonance Experiments. *Phys Rev.* 1954;94(3):630 - 638.
7. Deelchand DK, Henry P-G, Marjańska M. Effect of Carr-Purcell refocusing pulse trains on transverse relaxation times of metabolites in rat brain at 9.4 Tesla. *Magn Reson Med.* 2015;73(1):13-20.
8. Michaeli S, Garwood M, Zhu XH, et al. Proton T_2 relaxation study of water, N-acetylaspartate, and creatine in human brain using Hahn and Carr-Purcell spin echoes at 4T and 7T. *Magn Reson Med.* 2002;47(4):629-633.
9. Deelchand DK, Kantarci K, Öz G. Improved localization, spectral quality, and repeatability with advanced MRS methodology in the clinical setting. *Magn Reson Med.* 2018;79(3):1241-1250.
10. Terpstra M, Cheong I, Lyu T, et al. Test-retest reproducibility of neurochemical profiles with short-echo, single-voxel MR spectroscopy at 3T and 7T. *Magn Reson Med.* 2016;76(4):1083-1091.
11. van de Bank BL, Emir UE, Boer VO, et al. Multi-center Reproducibility of Short Echo Time Single Voxel 1H MRS of the Human Brain at 7T with Adiabatic Slice-Selective Refocusing Pulses. *Proc Intl Soc Mag Reson Med.* 2013:3982.
12. Bednařík P, Moheet A, Deelchand DK, et al. Feasibility and reproducibility of neurochemical profile quantification in the human hippocampus at 3 T. *NMR in Biomedicine.* 2015;28(6):685-693.
13. Deelchand DK, Adanyeguh IM, Emir UE, et al. Two-site reproducibility of cerebellar and brainstem neurochemical profiles with short-echo, single-voxel MRS at 3T. *Magn Reson Med.* 2015;73(5):1718-1725.
14. van de Bank BL, Emir UE, Boer VO, et al. Multi-center reproducibility of neurochemical profiles in the human brain at 7 Tesla. *NMR Biomed.* 2015;28(3):306-316.
15. Andronesi OC, Ramadan S, Ratai E-M, Jennings D, Mountford CE, Sorensen AG. Spectroscopic imaging with improved gradient modulated constant adiabaticity pulses on high-field clinical scanners. *J Magn Reson.* 2010;203(2):283-293.
16. Garwood M, DelaBarre L. The return of the frequency sweep: designing adiabatic pulses for contemporary NMR. *J Magn Reson.* 2001;153(2):155-177.
17. Warnking JM, Pike GB. Bandwidth-modulated adiabatic RF pulses for uniform selective saturation and inversion. *Magnetic Resonance in Medicine.* 2004;52(5):1190-1199.
18. Ordidge RJ, Wylezinska M, Hugg JW, Butterworth E, Franconi F. Frequency offset corrected inversion (FOCI) pulses for use in localized spectroscopy. *Magn Reson Med.* 1996;36(4):562-566.
19. Tannus A, Garwood M. Adiabatic pulses. *NMR Biomed.* 1997;10(8):423-434.
20. Tkáč I, Starčuk Z, Choi IY, Gruetter R. In vivo ^{1}H NMR spectroscopy of rat brain at 1 ms echo time. *Magn Reson Med.* 1999;41(4):649-656.

21. Schirmer T, Auer DP. On the reliability of quantitative clinical magnetic resonance spectroscopy of the human brain. *NMR in Biomedicine.* 2000;13(1):28-36.
22. Park YW, Deelchand DK, Joers JM, et al. AutoVOI: real-time automatic prescription of volume-of-interest for single voxel spectroscopy. *Magn Reson Med.* 2018;80(5):1787-1798.
23. Gruetter R. Automatic, localized in vivo adjustment of all first- and second-order shim coils. *Magn Reson Med.* 1993;29(6):804-811.
24. Gruetter R, Tkac I. Field mapping without reference scan using asymmetric echo-planar techniques. *Magn Reson Med.* 2000;43(2):319-323.
25. Landheer K, Juchem C. FAMASITO - FASTMAP Shim Tool Towards User-Friendly Single-Step B0 Homogenization. *Proc Intl Soc Mag Reson Med.* 2019;27:0216.
26. Landheer K, C J. FAMASITO - FASTMAP Shim Tool for Efficient B0 Shimming. 2018;Columbia Tech Ventures (CTV) License CU18208(innovation.columbia.edu/technologies/CU18208_famasito).
27. Noeske R, Toncelli A, Hlavata H, M T. Voxel Based Transmit Gain Calibration using Bloch-Siegert semi-LASER at 7T. *Proc Intl Soc Mag Reson Med.* 2017;25:5509.
28. Carlson JW, Kramer DM. Rapid radiofrequency calibration in MRI. *Magnetic Resonance in Medicine.* 1990;15(3):438-445.
29. MRspa: Magnetic Resonance signal processing and analysis https://www.cmrr.umn.edu/downloads/mrspa/ Aug 2018.
30. Natt O, Bezkorovaynyy V, Michaelis T, Frahm J. Use of phased array coils for a determination of absolute metabolite concentrations. *Magn Reson Med.* 2005;53(1):3-8.
31. Provencher SW. Estimation of metabolite concentrations from localized in vivo proton NMR spectra. *Magn Reson Med.* 1993;30(6):672-679.
32. CMRR Spectroscopy Package. https://www.cmrr.umn.edu/spectro/.
33. Deelchand DK, Auerbach EJ, Kobayashi N, Marjańska M. Transverse relaxation time constants of the five major metabolites in human brain measured in vivo using LASER and PRESS at 3 T. *Magn Reson Med.* 2018;79(3):1260-1265.

Table 1

Selected gradient-modulated refocusing RF pulses where the duration, bandwidth and modulations were empirically determined to achieve 98% magnetization inversion within a B_1 limit of 15 μT. Note that the standard hyperbolic secant HS4R25 pulse is an exception since it requires a B_1 of ~25 μT. The gradient factor represents the gradient strength in the middle of the RF pulse and the higher this number the lower the required B_1. For instance, a gradient factor of 85% means the center of the gradient is 15% of its maximum gradient selection value.

RF pattern	Duration (ms)	Bandwidth (kHz)	HS modulation	Gradient modulation	Gradient factor (%)	CSDE (%/ppm)
HS4R25	4	6.25	4	0	0	2.01
BASSI	4.5	10	-	-	-	1.01
FOCI	4.5	8.89	1	C-shaped	90	0.95
GOIA-HS	4.5	10	8	4	85	1.67
GOIA-WURST	4.5	10	16	4	85	1.33

Table 2

Assessment of RF pulses: Localization efficiency (L_{Eff}), contamination error (C_{Err}) and ripple artifacts (R_{PP}) measured inside and outside the VOI. R_{pp} is expressed as a % of Mz. Note that the HS4R25 was also included in the comparison; although this pulse has no ripple artifact outside the VOI compared to gradient-modulated pulses, its inversion efficiency was slightly lower than the other pulses.

	On-resonance					**200 Hz off-resonance**				
RF Pattern / Performance Metric	**HS4R 25**	**BASSI**	**FOCI**	**GOIA-HS**	**GOIA-WURST**	**HS4R25**	**BASSI**	**FOCI**	**GOIA-HS**	**GOIA-WURST**
L_{Eff} (%)	94.7	96.4	96.6	94.8	95.3	94	95.1	94.6	93.6	94.3
C_{Err} (%)	5.9	2.9	2.3	4.3	3.3	6.6	3.4	4	5.3	3.6
$R_{PP,inside}$ (% M_Z)	2.44	11.88	2.38	3.82	1.77	2.44	21.31	7.53	9.78	6.78
$R_{PP,outside}$ (% M_Z)	0	1.08	2.07	0.12	0.16	0	7.77	8.38	2.35	0.93